Supplementary Information

SI Figures and tables

Strengths and limitations of alternative methods for studying hydrological LUC effects, see Table S1**.** The most complex and coupled modelling approaches account for the highest number of feedback processes. However, the high degree of freedom also contribute to the high sensitivity of precipitation to initial conditions and the low signal-to-noise ratios. For example, a scenario replacing natural with present-day land cover only detected a significant response in less than 5 % of all grid cells in a single model analysis (Findell et al., 2007) and less than 5 % in non-perturbed grid cells across seven different models (Pitman et al., 2009). The challenges in simulating precipitation due to cloud formation, aerosol representation, and inherent uncertainties in circulation response (Aloysius et al., 2016; Koren et al., 2012; Shepherd, 2014), and non-closure of water balance in semi-coupled modelling approaches (Bring et al., 2015) also contribute to a high model dependence in estimates of river flow change from LUC (Kundzewicz et al., 2007). Thus, the sign, magnitude, and location of impacts vary widely among models (Aloysius et al., 2016; Pitman et al., 2009). Observation-based methods relate presence of vegetation or irrigation to precipitation or river flows using statistical methods, often in combination with moisture tracking to determine the geographical origin of rainfall (DeAngelis et al., 2010; Kustu et al., 2010, 2011; Spracklen et al., 2012). Limitations of this type of methods include variations in data quality, challenges in isolating effects of land-use from climate variability, and difficulties establishing causation from correlation (Matin and Bourque, 2015). Key elements missing in all approaches include socio-economic dynamics and landscape resilience, which are complex issues currently explored in experimental model settings (Nitzbon et al., 2017; Reyer et al., 2015).

Table S1. Methods for estimating land-use change impacts on rainfall or river flows.

Method	Key merits	Key limitations*	References
Earth System Model (ESM)	- Inclusion of multiple land-atmosphere-ocean feedbacks - Water balance closure	- Computationally costly. - Does not always include irrigation.	(Betts et al., 2015; Garcia et al., 2016)
General circulation model (GCM)	- Inclusion of multiple land-atmosphere-ocean feedbacks. (Sea surface temperature can be fixed to increase the signal-to-noise ratio.) - Coupled models close the water balance.	- Considerable noise in precipitation and runoff change (i.e., few grid cells passing significance test). - Does not always include irrigation. - Difficult to understand mechanisms. - Computationally costly.	(Bring et al., 2015; Findell et al., 2007; Pitman et al., 2009)
Regional climate model (RCM)	- Simulation of changes in convection and orographic precipitation - Can simulate enhanced local rainfall from deforested patches - Higher signal-to-noise ratio for precipitation change due to fixed boundary conditions	- Limitations in representing clouds - Potentially ignores water balance closure - No feedback across fixed regional boundaries	(Bagley et al., 2014; Lawrence and Vandecar, 2014)
Offline land surface model (LSM)	- Often includes irrigation.	- No land-atmosphere feedback. - No water balance closure.	(Gerten et al., 2008; Rost et al., 2008a, 2008b; Sterling et al., 2012)
Observations	- Observed	- Correlation rather than causation, thus, often combined with modelling. - Challenging attribution due to concurrent climate change and LUC	(Spracklen et al., 2012)
Meta-analysis	- Synthesis results from many different types of studies	- Limitation in spatially and temporally resolved estimates	(Spracklen and Garcia-Carreras, 2015)
Two-way coupled moisture recycling	- Includes irrigation - Phenology (LAI) responds to precipitation change	- Ignoring other types of land-atmosphere feedback.	This study, (Keys et al., 2016)

	- Water balance closure - Computationally efficient

*Limitations of most models in simulating vegetation feedback (e.g., rooting depth adjustment), disturbance processes (e.g., pathogens), and societal response (e.g., behavioural change) (Reyer et al., 2015).

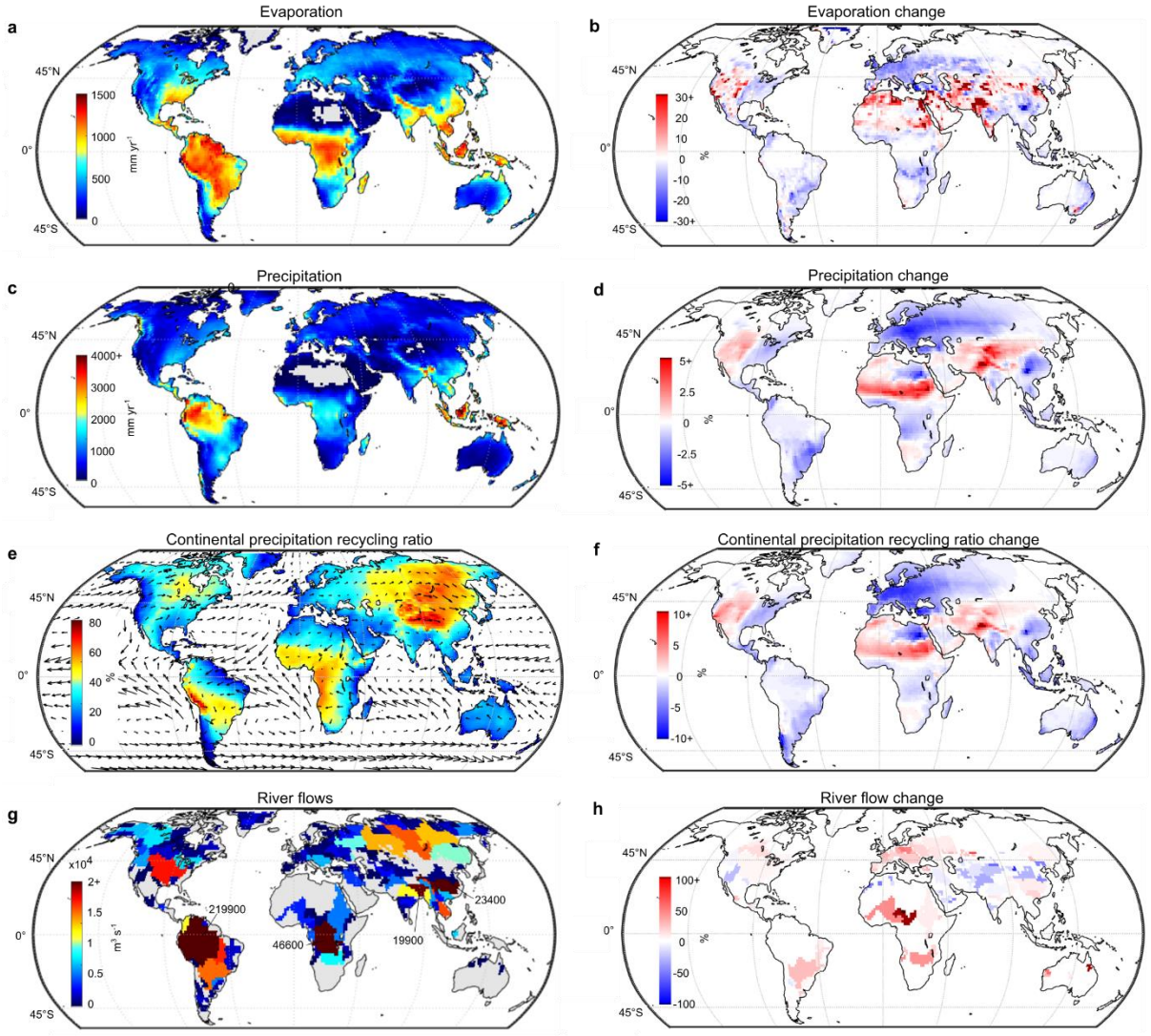

Figure S1. Land-use change induced changes in hydrological flows. a, Current evaporation, **b,** relative changes in evaporation **c,** current precipitation, **d,** relative change in precipitation, **e,** current continental precipitation recycling ratio (i.e., precipitation with terrestrial origin divided by total precipitation: $P_{tracked}/P$) where arrows show average winds in the lower atmosphere, **f,** relative change in continental precipitation recycling ratio, **g,** current river flow, and **h,** relative change in river flows. Values below about 0.5 % of maximum display value in **a, c, e,** and **g** are in grey.

Table S2. Overview of literature sources estimating human impact on river flows included in Fig. 2.

	Type	Time	Method	River flow change
LUC				
R08a(Rost et al., 2008a)	Pot - > Cur	1971-2000	Offline dynamic vegetation model LPJmL.	+1306 km^3 yr^{-1}
R08b(Rost et al., 2008b)	Pot - > Cur	1991-2000	Offline dynamic vegetation model LPJmL.	+1770 km^3 yr^{-1}
S12(Sterling et al., 2012)	Pot - > Cur	Mixed	Literature and statistical modelling in GIS.	+3500 km^3 yr^{-1}
S12(Sterling et al., 2012)	Pot - > Cur	1950-2000	Offline land surface model ORCHIDEE.	+3869 km^3 yr^{-1}
P07(Piao et al., 2007)	20th century	1901-1999	Offline land surface model ORCHIDEE.	+1089 km^3 yr^{-1}
G08(Gerten et al., 2008)	20th century	1901-2002	Offline dynamic vegetation model LPJmL. Trend from land-use change simulation using CRU precipitation.	+680 km^3 yr^{-1}
Climate change				
P07(Piao et al., 2007)	20th century	1901-1999	Offline land surface model ORCHIDEE. Climate change excluding CO_2 effect.	+1771 km^3 yr^{-1}
G08(Gerten et al., 2008)	20th century	1901-2002	Offline dynamic vegetation model LPJmL. Trend from precipitation P and temperature T change simulation using CRU precipitation.	+2600 km^3 yr^{-1} (P), -360 km^3 yr^{-1} (T), +2240 km^3 yr^{-1} (P+T)
A10(Alkama et al., 2010)	20th century	1901-2000	Offline land surface model ORCHIDEE. Climate change effect only.	+2477 km^3 yr^{-1}
CO_2 effect				
P07(Piao et al., 2007)	20th century	1901-1999	Offline land surface model ORCHIDEE. CO_2 allowing LAI change.	-545 km^3 yr^{-1}
G08(Gerten et al., 2008)	20th century	1901-2002	Offline dynamic vegetation model LPJmL. Trend from CO_2 simulation.	+480 km^3 yr^{-1}
A10(Alkama et al., 2010)	20th century	1901-2000	Offline land surface model ORCHIDEE. CO_2 effect only.	+275 km^3 yr^{-1}
Water consumption				
R08a(Rost et al., 2008a)	Pot - > Cur	1971-2000	Offline dynamic vegetation model LPJmL. Excluding nonlocal blue water (ILIM).	-457 km^3 yr^{-1}
G08(Gerten et al., 2008)	20th century	1901-2002	Offline dynamic vegetation model LPJmL. Trend from irrigation simulation.	-120 km^3 yr^{-1}
D09(Döll et al., 2009)	Pot - > Cur	2002	Offline hydrological model WaterGAP.	-1300-1400 km^3 yr^{-1}
S12(Sterling et al., 2012)	Pot - > Cur	Mixed	Literature review of withdrawal. Assuming water consumption to be 52 % of total withdrawal.	-1250 km^3 yr^{-1}
J15(Jaramillo and Destouni, 2015)	20th century	1901-1954 vs. 1955-2008	Analyses of hydroclimatic data for 100 large basins (35 % global land area).	-4370 km^3 yr^{-1} (±979 km^3 yr^{-1})
Overall human impact				
G08(Gerten et al., 2008)	20th century	1901-2002	Offline dynamic vegetation model LPJmL. Sum of precipitation, temperature, land-use change, CO_2, irrigation effect.	+3280 km^3 yr^{-1}
S12(Sterling et al., 2012)	Mixed	Mixed	Mean change from literature review.	+1500 km^3 yr^{-1}

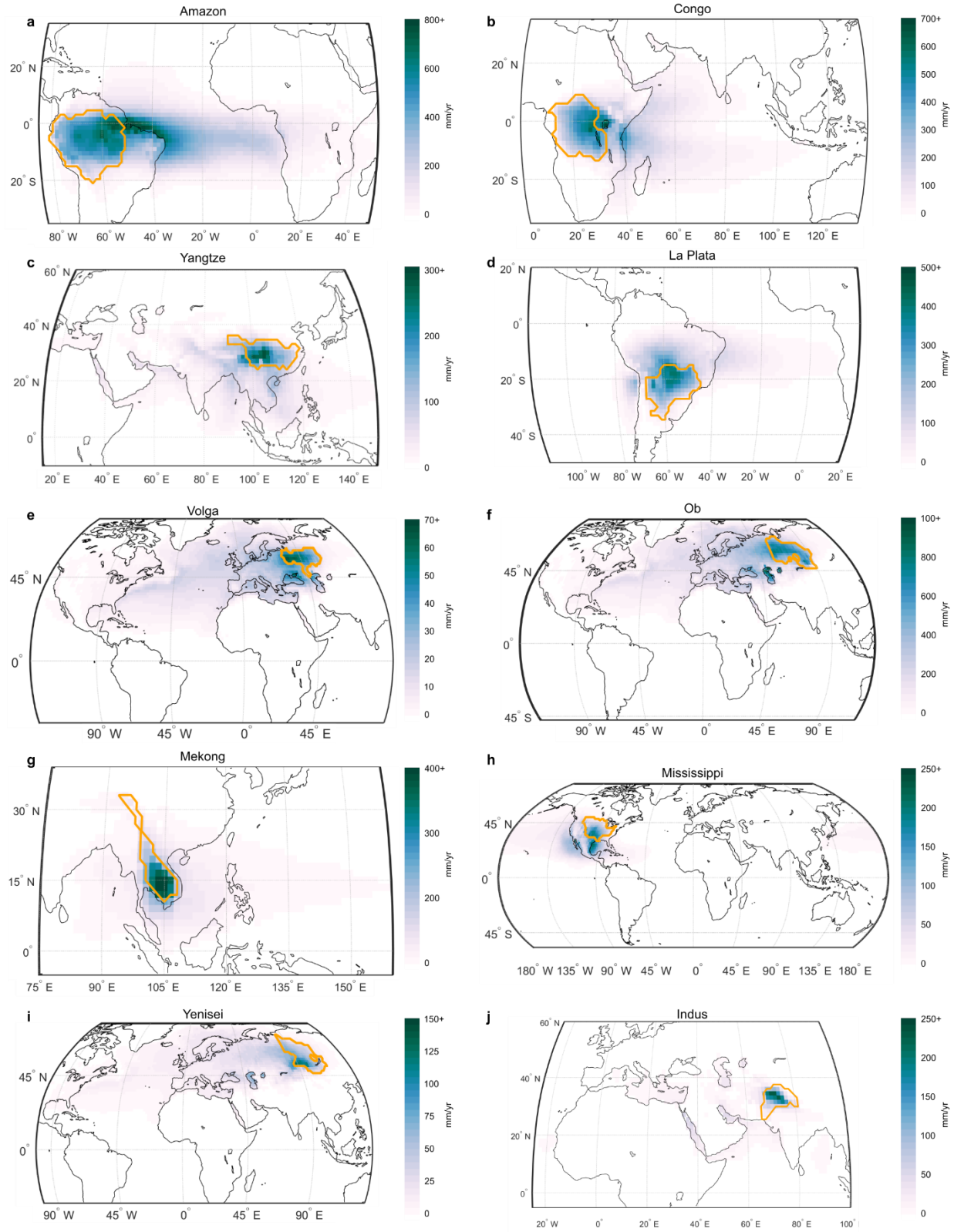

Figure S2. Mean annual precipitation sources for selected river basins (boundaries in orange).

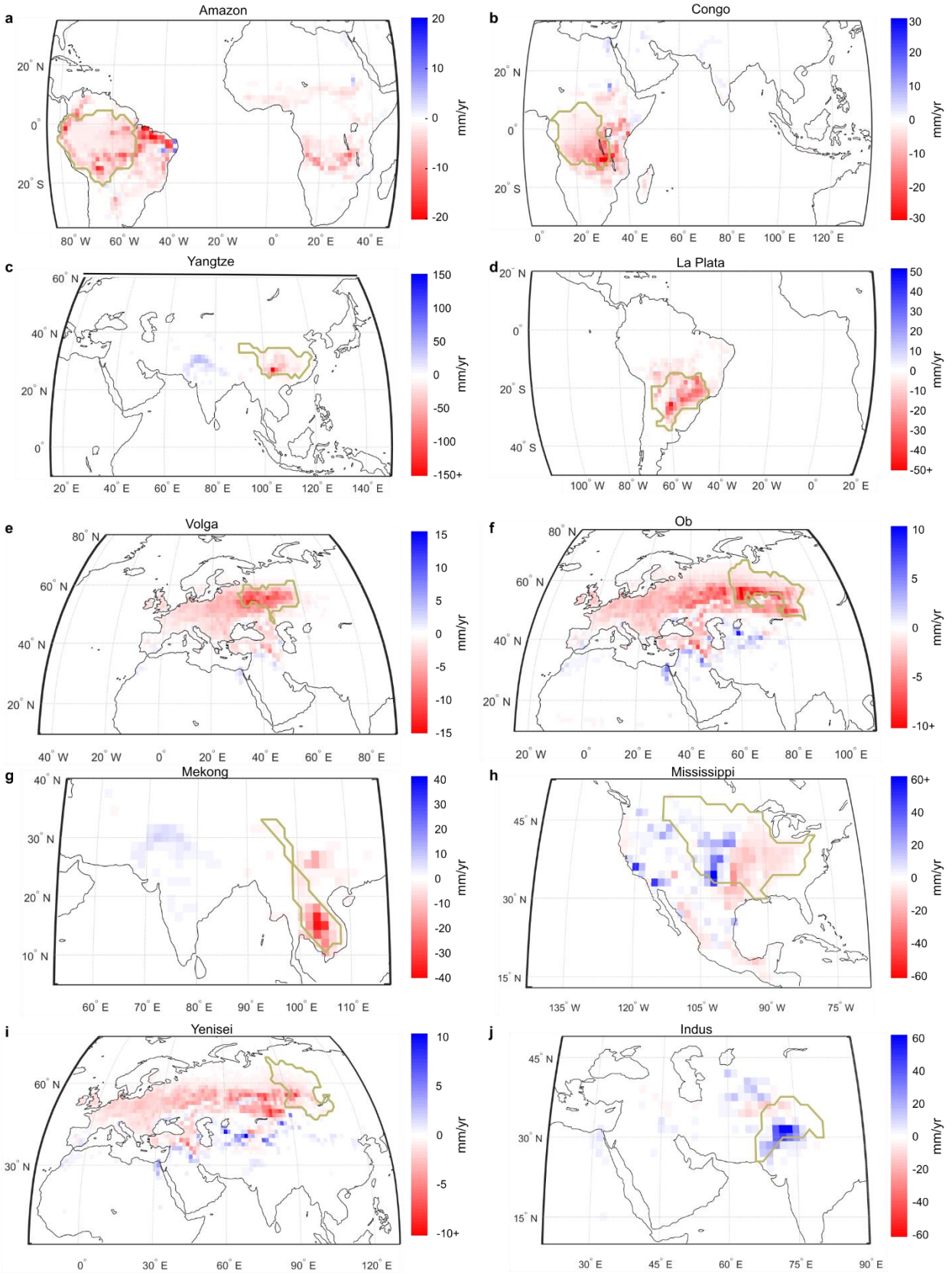

Figure S3. Impacts of human land-use change on mean annual precipitation source evaporation (i.e., ΔP_{import} + $\Delta P_{basin\text{-}recycling}$) for selected river basins (boundaries in dark yellow).

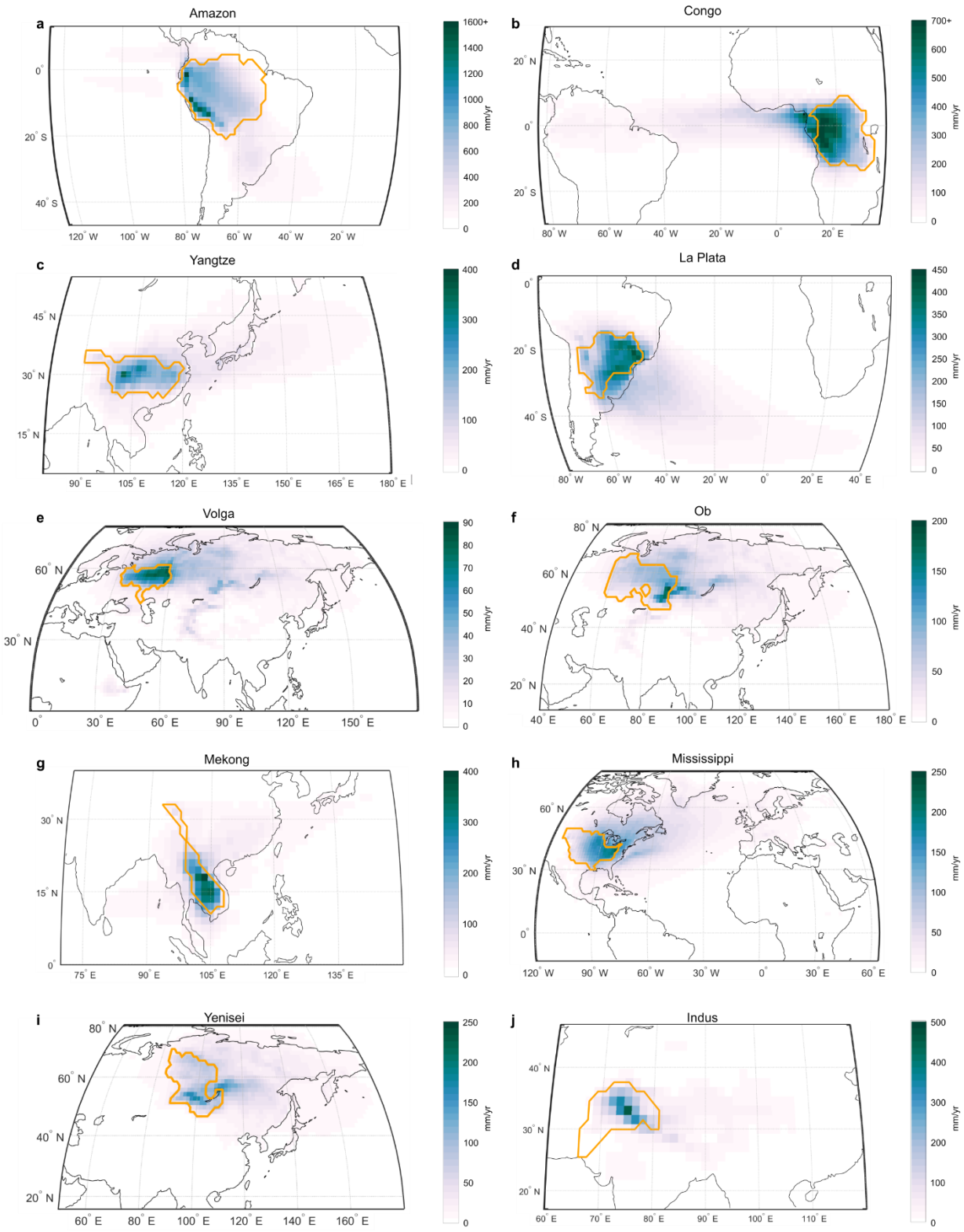

Figure S4. Mean annual evaporation sinks for selected river basins (boundaries in orange).

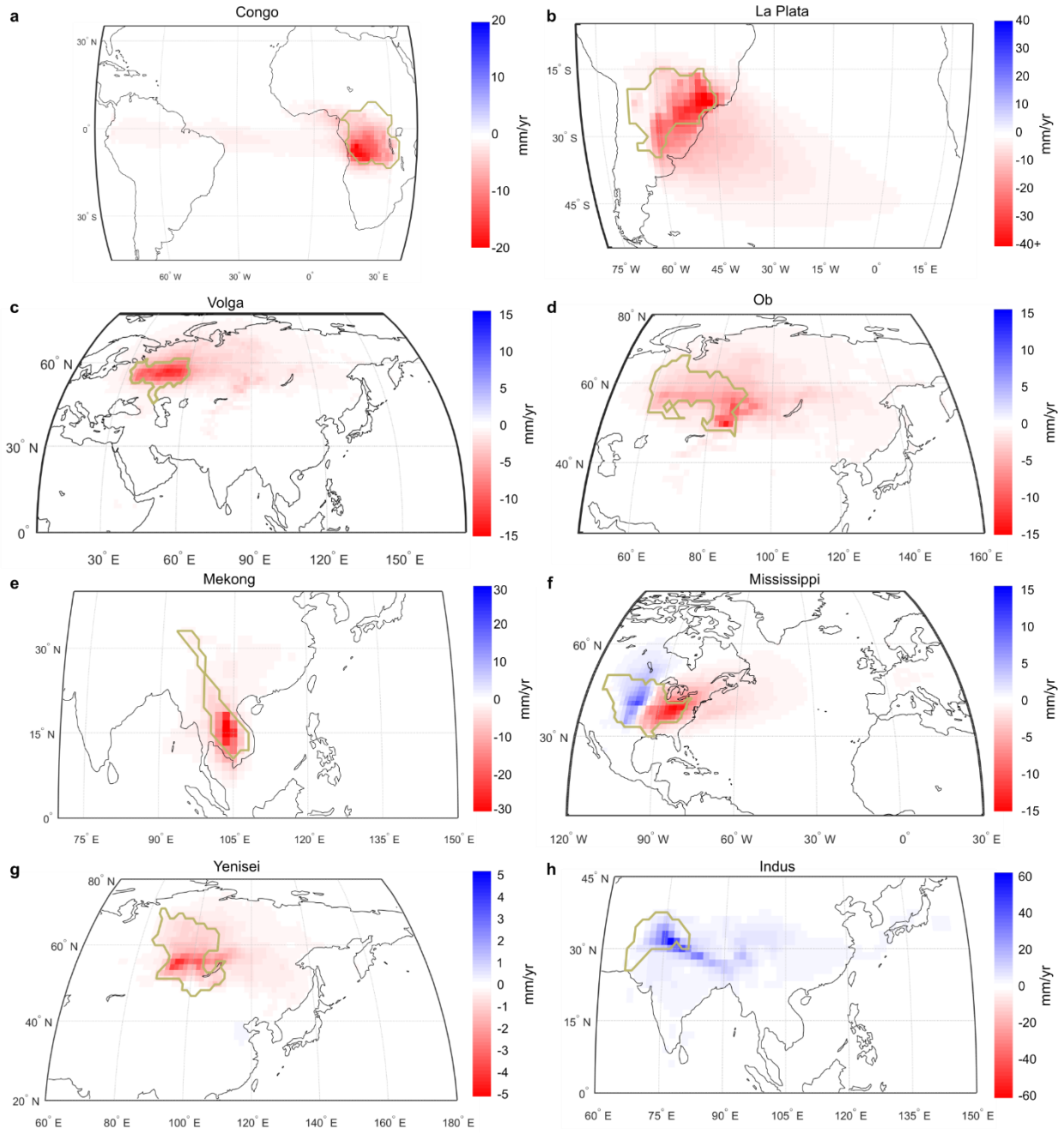

Figure S5. Impacts of human land-use change on mean annual evaporation sink (i.e., $\Delta P_{import} + \Delta P_{basin\text{-}recycling}$) for selected river basins (boundaries in dark yellow).

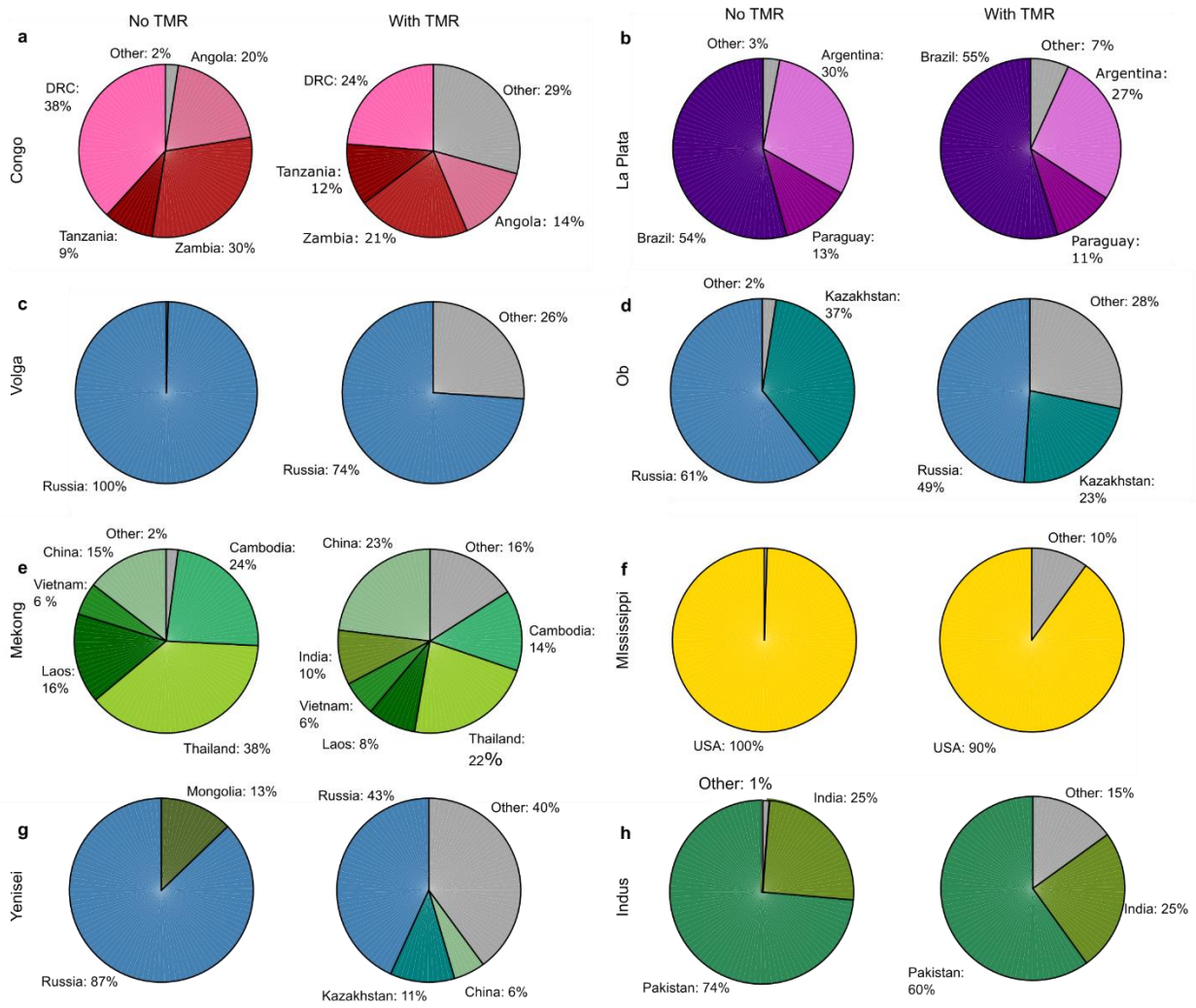

Figure S6. Nation influence on river flow change depending on whether terrestrial moisture recycling (TMR) is taken into account in **a**, La Plata; **b**, Volga; **c**, Ob; **d**, Mississippi; **e**, Yenisei; and **f**, Indus. Without considering TMR river flow change influence originates entirely from evaporation change within the basin. With consideration of TMR, nation influence to river flow change is considered as the sum of absolute changes in precipitation export and the sum of absolute changes in evaporation export (Methods). Single country contribution below 5 % is bundled into the category “Other”.

SI Materials and Methods

Moisture tracking scheme. Moisture is tracked using the Eulerian moisture tracking scheme Water Accounting Model-2 layers (WAM-2layers) (van der Ent, 2014; van der Ent et al., 2014). WAM-2layers tracks atmospheric moisture from zero pressure to surface pressure in two layers. Within the layers, atmosphere is assumed to be well-mixed. WAM-2layers tracks vapour flows by applying the water balance. For example, the following equation is used to track where evaporation from a given region falls as precipitation (i.e., forward tracking):

$$\frac{\partial S_{\text{tracked}}}{\partial t} = \frac{\partial \left(S_{\text{tracked}} u \right)}{\partial x} + \frac{\partial \left(S_{\text{tracked}} v \right)}{\partial y} + E_{\text{tracked}} - P_{\text{tracked}} \pm F_{\text{vertical,tracked}}$$

where S_{tracked} is the tracked atmospheric storage in an atmospheric column in one layer, t is time, u and v are wind components in the x zonal and y meridional direction, E_{tracked} is tracked evaporation entering and P_{tracked} is precipitation exiting an atmospheric column and layer, and $F_{\text{vertical,tracked}}$ is the tracked vertical moisture transport between the two layers. An analogous equation is used for tracking the source of precipitation to a given region (i.e., backward tracking). The spatial resolution of WAM-2layers is 1.5^{o} and input data are linearly interpolated to the 15 minute time step to maintain numerical stability. WAM-2layers has been employed previously for analysing atmospheric moisture transport over terrestrial areas (Keys et al., 2012, 2016) and validated against other types of moisture tracking algorithms (Van Der Ent et al., 2013). We used the MATLAB (The MathWorks, n.d.) version of WAM-2layers, but a Python version is also openly available on Github (van der Ent, 2016).

Hydrological model. Evaporation is simulated by the process-based hydrological model Simple Terrestrial Evaporation to Atmosphere Model (STEAM)(Wang-Erlandsson et al., 2014). STEAM partitions evaporation into five fluxes: vegetation interception, floor interception, transpiration, soil moisture evaporation, and open-water evaporation. STEAM uses the Penman-Monteith equation (Monteith, 1965) to estimate potential evaporation, the Jarvis-Stewart equation (Stewart, 1988) to compute surface stomatal resistance, and Jolly's growing season index (function of minimum temperature, soil moisture content, and daylight) to describe phenology (Jolly et al., 2005). STEAM operates at 1.5^{o} x 1.5^{o} and a 3 hour resolution. Based on the long term water balance, mean annual river flow is assumed to approximately equal the difference between mean annual precipitation and evaporation. STEAM was validated in previous studies (Wang-Erlandsson et al., 2014, 2016) and compared well with recent observation based analyses of evaporation partitioning by land-cover type (Wei et al., 2017). Validation against observed runoff data is further performed and shown in Figure S8**.**

Modifications from the original version of STEAM (Wang-Erlandsson et al., 2014, 2016) includes: (1) update of land use classification and parameterisation (Table S3), (2) development of a mosaic-tile approach for faster computation (described below), (3) use of a temperature threshold of 0^{o}C for differentiating snowfall from rainfall, and (4) differences in input data (i.e., root zone storage capacity, land surface map, precipitation data source as described in Data).

In the original version of STEAM (Wang-Erlandsson et al., 2014, 2016), each land cover (L) is simulated for the whole world ("mosaic"), and the total terrestrial evaporation (E) is obtained by weighing each land cover's evaporation (E_L) by its fractional spatial occupation (φ_L): $E = \Sigma E_L \varphi_L$. In the coupled version of STEAM-WAM, we instead weigh each land cover specific parameter (p_L) with the land cover fractional occupation within each group of land-use or land-cover type. This merged land

cover parametrisation map (p) is then used to simulate total evaporation ("mosaic-tile"): $E(p) = E(\Sigma p_L \varphi_L)$.

Coupling of moisture tracking scheme and the hydrological model. Current land use scenarios do not require iterative model coupling, since present day hydrological flows can be represented by current data and simulation. To obtain evaporation and precipitation under potential land cover, STEAM is coupled with WAM-2layers by (1) simulating present day evaporation in STEAM and forward tracking terrestrial evaporation with WAM-2layers, (2) simulating evaporation in STEAM based on present day precipitation and potential land cover, and forward track the fate of terrestrial evaporation with WAM-2layers, (3) calculating the change in tracked precipitation, (4) updating the present day precipitation with the changes in tracked precipitation, and (5) simulating evaporation in STEAM based on updated precipitation and potential land cover, and forward tracking the fate of terrestrial evaporation with WAM-2layers, see Figure S9. Steps 3-5 are iterated until the annual precipitation change is below 1 % and the monthly precipitation change is below 5 mm month^{-1} in every grid cell, which ultimately resulted in four iterations in total. This procedure assumes that land-use induced changes in terrestrial evaporation will result in proportional changes in precipitation with terrestrial origin.

Direct comparison of simulation results between this study and other General Circulation Model (GCM) studies as evaluation are complicated by the fact that GCM studies have shown widely different results with very low signal-to-noise ratio for LUC-induced precipitation change (Pitman et al., 2009). Regional deforestation scenarios generate higher ratios of significant results near the source of change, albeit noise remains high in distant regions (Werth and Avissar, 2002). Meta-analysis of 96 different GCM and (Regional Climate Model) RCM deforestation simulations shows that precipitation change vary widely among models (Spracklen and Garcia-Carreras, 2015). Under 10 % conversion of Amazon forest to pasture or soybean production, the interquartile range of rainfall change in the Amazon basin is 0 to -4 % (Spracklen and Garcia-Carreras, 2015). As comparison, the STEAM-WAM2layers approach with change from potential to current land-use change (i.e., 8.8 % deforestation extent in the Amazon), causes a rainfall reduction of 0.4 % in the Amazon and thus falls in the conservative range.

Meteorological data. Meteorological data were primarily taken from Earth Retrospective Analysis Interim (ERA-I) from European Centre for Medium-Range Weather Forecasts (ECMWF) (Dee et al., 2011). ERA-I meteorological forcing to STEAM are: snowmelt, temperature at 2m height, dew point temperature at 2m height, wind speed (meridional and zonal vectors) at 10 m height, incoming shortwave radiation, and net longwave radiation. In addition, ERA-I evaporation data were used to downscale calculated daily potential evaporation in STEAM to the 3 hour time step. ERA-I model level forcings used in the WAM-2layers are specific humidity, and wind speed at 6 hourly resolution, spanning from zero to surface pressure. In addition, 3 hourly ocean evaporation is taken from ERA-I. The Modern-Era Retrospective analysis for Research and Applications (MERRA) reanalysis has also been used as input to WAM-2layers for comparison. Both reanalyses datasets generated similar persistent moisture recycling patterns, except in South America where differences arise due to underestimation of precipitation in MERRA (Keys et al., 2014).

Since river flow estimates can be highly sensitive to precipitation (Biemans et al., 2009; Fekete et al., 2004), we force WAM-2layers and STEAM with the state-of-the-art precipitation product Multi-Source Weighted-Ensemble Precipitation (MSWEP) (Beck et al., 2017) that was specifically created for hydrological modelling. The long-term mean of MSWEP is based on CHPclim and more accurate regional datasets are used where available. The temporal variability is based on two gauge based, three satellite based, and two reanalysis datasets, where the contribution to the MSWEP dataset is

determined by the data quality assessed through time and space. The use of MSWEP as forcing for STEAM resulted in runoff estimates that compare well to observed runoff data (Figure S8).

Runoff data used for benchmarking were taken from the composite (observed river discharge consistent with water balance model) from the Global Runoff Data Centre (GRDC) (Fekete et al., 2002). The separate GRDC water balance model runoff fields are included in the comparison for reference (Figure S8)**.**

Land data. Land use and land cover data input to STEAM are primarily based on the Ramankutty potential land-cover (Ramankutty and Foley, 1999) and current land-use scenarios from ref. (Ramankutty et al., 2008) for consistency. We further added permanent wetlands, permanent snow or ice, and urban or built-up areas from the Land Cover Type Climate Modeling Grid (CMG) MCD12C1 International Geosphere Biosphere Program (IGBP) land classification created from Terra and Aqua Moderate Resolution Imaging Spectroradiometer (MODIS) data (Friedl et al., 2010) for the year 2005. Finally, monthly irrigated rice and irrigation non-rice crops were obtained from the data set of Monthly Irrigated and Rainfed Crop Areas around the year 2000 (MIRCA2000) V1.1. (Portmann et al., 2010). The urban and irrigated areas were only added to the current land cover map. In this merging procedure, MODIS is allowed to override the Ramankutty datasets, and MIRCA2000 is allowed to override the Ramankutty map as long as it does not extend over the cropland areas.

The root zone storage capacity map is based on a climate-observation based root zone storage capacity (S_R)(Wang-Erlandsson et al., 2016) derived from satellite and energy balance based evaporation, gauge-based precipitation, and modelled irrigation. The best performing Gumbel normalised root zone storage capacity ($S_{R,CRU\text{-}SM,merged}$) was used. Root zone storage capacity for both current and potential land-cover and land-use scenarios were constructed from mean of land-cover type and Köppen-Geiger climate class (Kottek et al., 2006). The mean root zone storage capacity of single land-cover types was used only in places where the combination of land-cover type and climate zone that exists in the potential land-cover scenario did not exist in the current land-use map.

Literature review of anthropogenic impacts on river flows. Literature sources included in Fig. 2 are either global studies of potential land cover to current land use, or transient studies of river flow changes over the 20th century. Studies without global coverage are not included in the comparison, e.g., Gedney et al., (2006), Findell et al. (2007), Alkama et al. (2013), Labat et al. (2004), and Dai et al. (2009) are excluded due to smaller land areas than other studies included. The results of Labat et al. (2004) have also been contested by later studies (Alkama et al., 2011; Legates et al., 2005; Milliman et al., 2008). Dai et al. (2009) also only covers river flow changes 1948-2004. We do not assume evaporation change to correspond to river flow change, unless authors explicitly endorse the translation. This excludes for example Gordon et al. (2005) and Boisier et al. (2014) from the inter-comparison.

Table S3. Land-cover and land-use parameterisation in STEAM.

	Group	LAI_{max}	LAI_{min}	α	h_{max}	h_{min}	z_{0g}	$r_{st,min}$
Unit		-	-	-	m	m	m	s m^{-1}
01: Water (Wa)	I – W	0	0	0.08	0	0	0.00137	0
02: Tropical evergreen forest/woodland (TrE)	II – F	5.5	5	0.20	30	30	0.02	200
03: Tropical deciduous forest/woodland (TrD)	II – F	5.5	1	0.18	30	30	0.02	200
04: Temp. broadleaf evergreen forest/woodland (TeB)	II – F	5.5	2	0.18	25	25	0.02	200
05: Temp. needleleaf evergreen forest/woodland (TeN)	II – F	5.5	2	0.15	17	17	0.02	300
06: Temp. deciduous forest/Woodland (TeD)	II – F	5.5	0.5	0.18	25	25	0.02	200
07: Boreal evergreen forest/Woodland (BoE)	II – F	5.5	2	0.15	17	17	0.02	300
08: Boreal deciduous forest/Woodland (BoD)	II – F	5.5	0.5	0.18	25	25	0.02	200

09: Evergreen/Deciduous Mixed Forest/Woodland (Mix)	II – F	5	1	0.17	20	20	0.02	250
10: Savanna (Sav)	III – S	2	0.5	0.25	0.8	0.1	0.02	150
11: Grassland/Steppe (Gra)	III – S	2	0.5	0.25	0.8	0.05	0.01	110
12: Dense Shrubland (DShr)	III – S	2.5	1	0.2	1.5	1.5	0.02	200
13: Open shrubland (OShr)	III – S	1.5	0.5	0.15	1	1	0.02	200
14:Tundra (Tun)	IV – B	2	1	0.15	0.8	0.1	0.01	80
15 Desert (Des)	IV – B	0.1	0	0.25	0.4	0	0.001	200
16 Polar desert/rock/ice (Ice)	IV – B	0	0	0.70	0	0	0.001	0
17: Wetland (Wet)	V – O	4	1	0.15	1	0.05	0.01	150
18: Urban (Urb)	IV – B	1	0.1	0.18	0.8	0	0.001	250
19: Pasture (Pas)	III – S	2	0.5	0.22	0.8	0.05	0.01	150
20: Rainfed cropland (RfCro)	VI – C	3.5	0.5	0.22	0.8	0.05	0.005	150
21: irrigated crop (IrCro)	VII – I	3.5	3.5	0.22	0.8	0.8	0.005	150
22: Irrigated rice (IrRic)	VIII - R	3.5	3.5	0.22	0.8	0.8	0.005	150

LAI_{max} is the maximum leaf area index, LAI_{min} is the minimum leaf area index, α is the albedo, h_{max} is the maximum plant height, h_{min} is the minimum plant height, z_{0g} is the ground roughness, and $r_{st,min}$ is the minimum stomatal resistance.

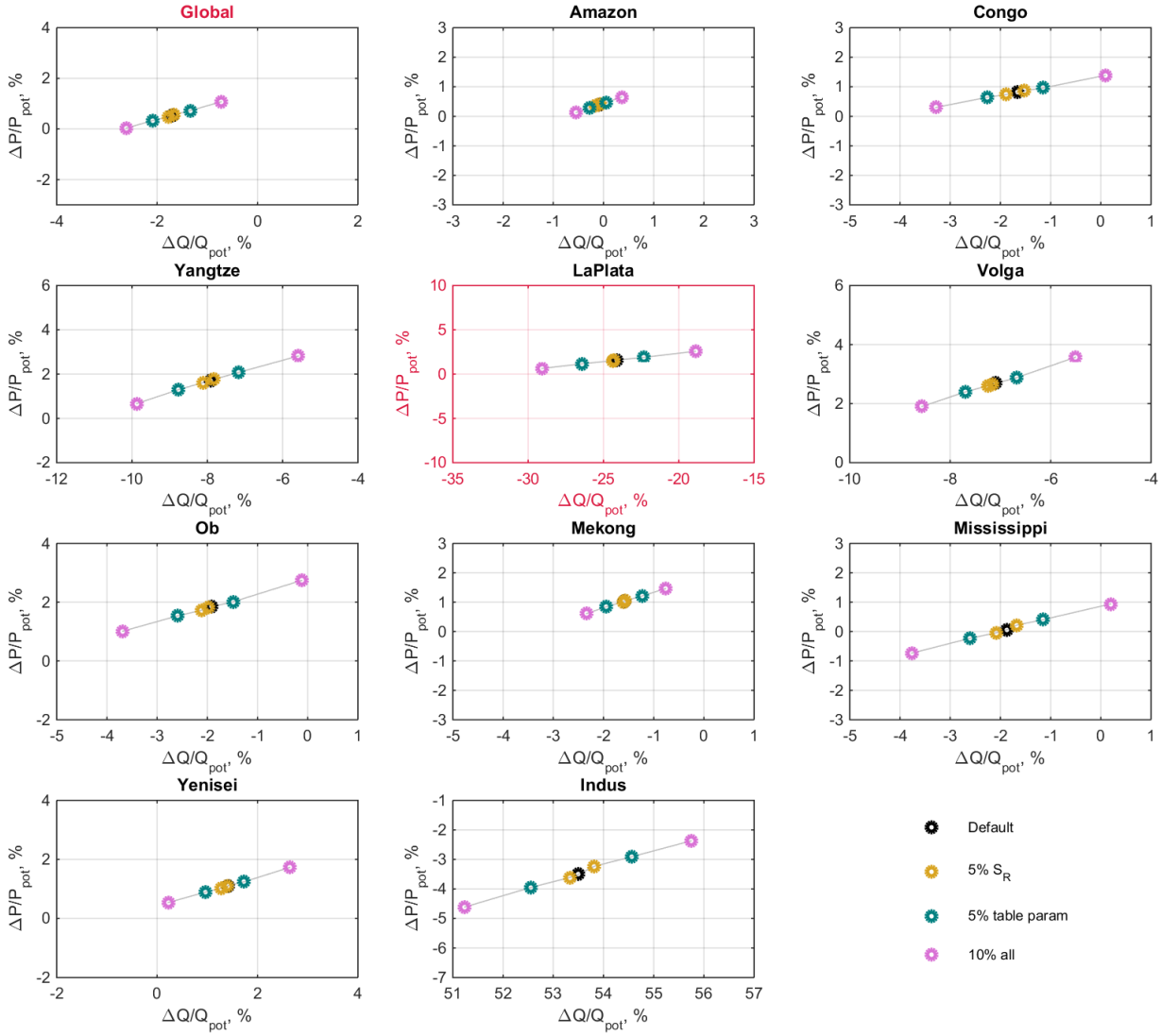

Figure S7. Sensitivity analysis. The relationship between annual mean precipitation change and river flow change under different perturbations of STEAM parameter values in pasture and croplands. The three different sets of perturbation experiments are: 5 % increase and decrease of root zone storage capacity S_R (green circles), 5% perturbation of six tabulated land parameters in a direction that causes either increase or decrease in evaporation (blue circles), and 10 % perturbation of both S_R and the six tabulated land parameters in a direction that causes either increase or decrease in evaporation (purple circles). Note that in each experiment, the parameter values are perturbed in the same direction in terms of increase or decrease in evaporation. The six look-up table parameters are maximum leaf area index LAI_{max}, minimum leaf area index LAI_{min}, albedo α, maximum plant height h_{max}, minimum plant height h_{min}, and minimum stomatal

resistance $r_{st,min}$. Except for La Plata, the different plots have identical scales and can therefore be compared to each other. Evaporation simulation in Mississippi and Indus can be slightly sensitive to initial soil moisture conditions (not shown). Presented results are from simulations for the years 2000-2002.

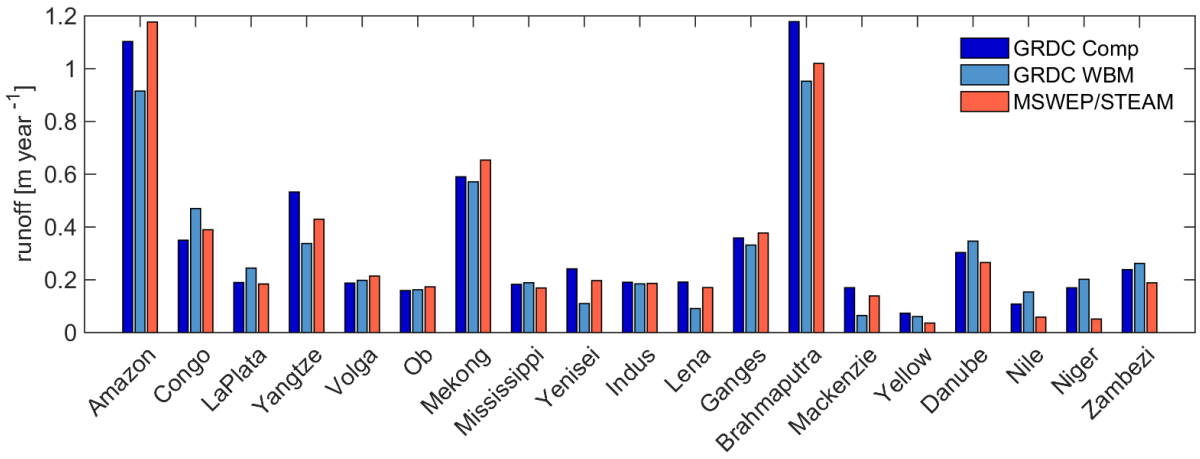

Figure S8. River flow validation. Comparison of simulated runoff (MSWEP/STEAM) with GRDC composite (GRDC Comp) and water balance model (GRDC WBM) runoff. MSWEP/STEAM deviates less from GRDC Comp (standard deviation σ = 0.0622 m yr^{-1}) than GRDC WBM (σ = 0.09993 m yr^{-1}).

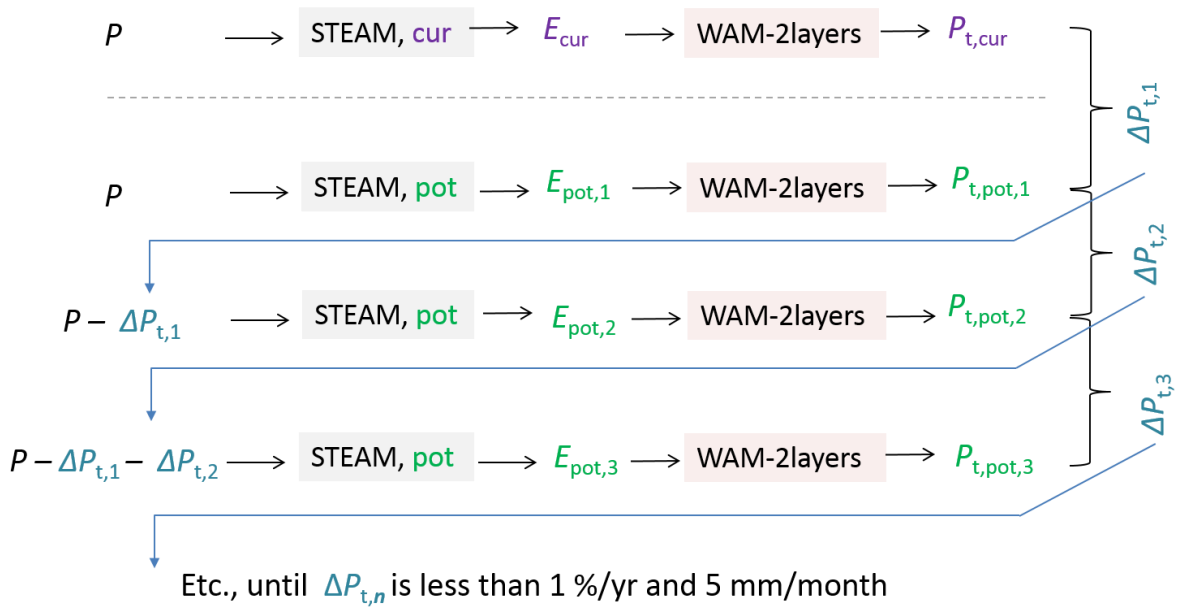

Figure S9. Model coupling schematic. Model coupling between STEAM and WAM-2layers based on current land use and potential land cover scenarios. *P* stands for current precipitation, *E* stands for evaporation. Subscript $_t$ stands for terrestrial origin, $_{pot}$ denotes simulation with potential land cover, $_{cur}$ denotes simulation with current land use, and $_n$ stands for the number of iterations.

SI references

Alkama, R., Kageyama, M. and Ramstein, G.: Relative contributions of climate change, stomatal closure, and leaf area index changes to 20th and 21st century runoff change: A modelling approach using the Organizing Carbon and Hydrology in Dynamic Ecosystems (ORCHIDEE) land surface model, J. Geophys. Res. Atmos., 115(17), D17112, doi:10.1029/2009JD013408, 2010.

Alkama, R., Decharme, B., Douville, H. and Ribes, A.: Trends in Global and Basin-Scale Runoff over the Late Twentieth Century: Methodological Issues and Sources of Uncertainty, J. Clim., 24(12), 3000–3014, doi:10.1175/2010JCLI3921.1, 2011.

Alkama, R., Marchand, L., Ribes, A. and Decharme, B.: Detection of global runoff changes: results from observations and CMIP5 experiments, Hydrol. Earth Syst. Sci., 17(7), 2967–2979, doi:10.5194/hess-17-2967-2013, 2013.

Aloysius, N. R., Sheffield, J., Saiers, J. E., Li, H. and Wood, E. F.: Evaluation of historical and future simulations of precipitation and temperature in central Africa from CMIP5 climate models, J. Geophys. Res. Atmos., 121(1), 130–152, doi:10.1002/2015JD023656, 2016.

Bagley, J. E., Desai, A. R., Harding, K. J., Snyder, P. K. and Foley, J. a.: Drought and Deforestation: Has land cover change influenced recent precipitation extremes in the Amazon?, J. Clim., 27, 345–361, doi:10.1175/JCLI-D-12-00369.1, 2014.

Beck, H. E., van Dijk, A. I. J. M., Levizzani, V., Schellekens, J., Miralles, D. G., Martens, B. and de Roo, A.: MSWEP: 3-hourly 0.25 degree global gridded precipitation (1979-2015) by merging gauge, satellite, and reanalysis data, Hydrol. Earth Syst. Sci., 21(1), 589–615, doi:10.5194/hess-21-589-2017, 2017.

Betts, R. A., Golding, N., Gonzalez, P., Gornall, J., Kahana, R., Kay, G., Mitchell, L. and Wiltshire, A.: Climate and land use change impacts on global terrestrial ecosystems and river flows in the HadGEM2-ES Earth system model using the representative concentration pathways, Biogeosciences, 12(5), 1317–1338, doi:10.5194/bg-12-1317-2015, 2015.

Biemans, H., Hutjes, R. W. a., Kabat, P., Strengers, B. J., Gerten, D. and Rost, S.: Effects of Precipitation Uncertainty on Discharge Calculations for Main River Basins, J. Hydrometeorol., 10(4), 1011–1025, doi:10.1175/2008JHM1067.1, 2009.

Boisier, J. P., De Noblet-Ducoudré, N. and Ciais, P.: Historical land-use-induced evapotranspiration changes estimated from present-day observations and reconstructed land-cover maps, Hydrol. Earth Syst. Sci., 11(9), 2045–2089, doi:10.5194/hessd-11-2045-2014, 2014.

Bring, A., Asokan, S. M., Jaramillo, F., Jarsjö, J., Levi, L., Pietroń, J., Prieto, C., Rogberg, P. and Destouni, G.: Implications of freshwater flux data from the CMIP5 multimodel output across a set of Northern Hemisphere drainage basins, Earth's Futur., 3(6), 206–217, doi:10.1002/2014EF000296, 2015.

Dai, A., Qian, T., Trenberth, K. E. and Milliman, J. D.: Changes in continental freshwater discharge from 1948 to 2004, J. Clim., 22(10), 2773–2792, doi:10.1175/2008JCLI2592.1, 2009.

DeAngelis, A., Domínguez, F., Fan, Y., Robock, A., Kustu, M. D. and Robinson, D.: Evidence of enhanced precipitation due to irrigation over the Great Plains of the United States, J. Geophys. Res., 115(D15), D15115, doi:10.1029/2010JD013892, 2010.

Dee, D., Uppala, S., Simmons, A. J., Berrisford, P., Poli, P., Kobayashi, S., Andrae, U., Balmaseda, M., Balsamo, G., Bauer, P., Bechtold, P., Beljaars, A. C. M., van de Berg, L., Bidlot, J., Bormann, N., Delsol, C., Dragani, R., Fuentes, M., Geer, A., Haimberger, L., Healy, S., Hersbach, H., Hólm, E., Isaksen, L., Kållberg, P., Köhler, M., Matricardi, M., McNally, A., Monge-Sanz, B., Morcrette, J.-J., Park, B.-K.,

Peubey, C., de Rosnay, P., Tavolato, C., Thépaut, J.-N. and Vitart, F.: The ERA-Interim reanalysis: configuration and performance of the data assimilation system, Q. J. R. Meteorol. Soc., 137, 553–597, doi:10.1002/qj.828, 2011.

Döll, P., Fiedler, K. and Zhang, J.: Global-scale analysis of river flow alterations due to water withdrawals and reservoirs, Hydrol. Earth Syst. Sci., 13(12), 2413–2432, doi:10.5194/hess-13-2413-2009, 2009.

van der Ent, R. J.: A new view on the hydrological cycle over continents, Delft University of Technology., 2014.

van der Ent, R. J.: WAM2layersPython, 2016.

van der Ent, R. J., Wang-Erlandsson, L., Keys, P. W. and Savenije, H. H. G.: Contrasting roles of interception and transpiration in the hydrological cycle – Part 2: Moisture recycling, Earth Syst. Dyn., 5(2), 471–489, doi:10.5194/esd-5-471-2014, 2014.

Van Der Ent, R. J., Tuinenburg, O. A., Knoche, H. R., Kunstmann, H. and Savenije, H. H. G.: Should we use a simple or complex model for moisture recycling and atmospheric moisture tracking?, Hydrol. Earth Syst. Sci., 17(12), 4869–4884, doi:10.5194/hess-17-4869-2013, 2013.

Fekete, B., Vörösmarty, C., Roads, J. and Willmott, C.: Uncertainties in precipitation and their impacts on runoff estimates, J. Clim., 17, 294–304, doi:10.1175/1520-0442(2004)017<0294:UIPATI>2.0.CO;2, 2004.

Fekete, B. M., Vörösmarty, C. J. and Grabs, W.: High-resolution fields of global runoff combining observed river discharge and simulated water balances, Global Biogeochem. Cycles, 16(3), 15-1-15–10, doi:10.1029/1999GB001254, 2002.

Findell, K. L., Shevliakova, E., Milly, P. C. D., Stouffer, R. J., Findell, K. L., Shevliakova, E., Milly, P. C. D. and Stouffer, R. J.: Modeled Impact of Anthropogenic Land Cover Change on Climate, J. Clim., 20(14), 3621–3634, doi:10.1175/JCLI4185.1, 2007.

Friedl, M. a., Sulla-Menashe, D., Tan, B., Schneider, A., Ramankutty, N., Sibley, A. and Huang, X.: MODIS Collection 5 global land cover: Algorithm refinements and characterization of new datasets, Remote Sens. Environ., 114(1), 168–182, doi:10.1016/j.rse.2009.08.016, 2010.

Garcia, E. S., Swann, A. L. S., Villegas, J. C., Breshears, D. D., Law, D. J., Saleska, S. R. and Stark, S. C.: Synergistic ecoclimate teleconnections from forest loss in different regions structure global ecological responses, edited by S. Joseph, PLoS One, 11(11), e0165042, doi:10.1371/journal.pone.0165042, 2016.

Gedney, N., Cox, P. M., Betts, R. A., Boucher, O., Huntingford, C. and Stott, P. A.: Detection of a direct carbon dioxide effect in continental river runoff records, Nature, 439(7078), 835–838, doi:10.1038/nature04504, 2006.

Gerten, D., Rost, S., von Bloh, W. and Lucht, W.: Causes of change in 20th century global river discharge, Geophys. Res. Lett., 35(20), L20405, doi:10.1029/2008GL035258, 2008.

Gordon, L. J., Steffen, W., Jönsson, B. F., Folke, C., Falkenmark, M., Johannessen, A. and Johannessen, Å.: Human modification of global water vapor flows from the land surface., Proc. Natl. Acad. Sci. U. S. A., 102(21), 7612–7617, doi:10.1073/pnas.0500208102, 2005.

Jaramillo, F. and Destouni, G.: Local flow regulation and irrigation raise global human water consumption and footprint, Science, 350(6265), 1248–1251, doi:10.1126/science.aad1010, 2015.

Jolly, W. M., Nemani, R. and Running, S. W.: A generalized, bioclimatic index to predict foliar phenology in response to climate, Glob. Chang. Biol., 11(4), 619–632, doi:10.1111/j.1365-

2486.2005.00930.x, 2005.

Keys, P. W., van der Ent, R. J., Gordon, L. J., Hoff, H., Nikoli, R. and Savenije, H. H. G.: Analyzing precipitationsheds to understand the vulnerability of rainfall dependent regions, Biogeosciences, 9(2), 733–746, doi:10.5194/bg-9-733-2012, 2012.

Keys, P. W., Barnes, E. A., van der Ent, R. J. and Gordon, L. J.: Variability of moisture recycling using a precipitationshed framework, Hydrol. Earth Syst. Sci., 18(10), 3937–3950, doi:10.5194/hess-18-3937-2014, 2014.

Keys, P. W., Wang-Erlandsson, L. and Gordon, L. J.: Revealing Invisible Water: Moisture Recycling as an Ecosystem Service., PLoS One, 11(3), e0151993, doi:10.1371/journal.pone.0151993, 2016.

Koren, I., Altaratz, O., Remer, L. A., Feingold, G., Martins, J. V. and Heiblum, R. H.: Aerosol-induced intensification of rain from the tropics to the mid-latitudes, Nat. Geosci., 5(2), 118–122, doi:10.1038/ngeo1364, 2012.

Kottek, M., Grieser, J., Beck, C., Rudolf, B. and Rubel, F.: World Map of the Köppen-Geiger climate classification updated, Meteorol. Zeitschrift, 15(3), 259–263, doi:10.1127/0941-2948/2006/0130, 2006.

Kundzewicz, Z. W., Mata, L. J., Arnell, N. W., Döll, P., Kabat, P., Jiménez, B., Miller, K. A., Oki, T., Sçen, Z. and Shiklomanov, I. A.: Freshwater resources and their management, edited by M. L. Parry, O. F. Canziani, J. P. Palutikof, P. J. van der Linden, and C. E. Hansen, Cambridge University Press, Cambridge, UK., 2007.

Kustu, M. D., Fan, Y. and Robock, A.: Large-scale water cycle perturbation due to irrigation pumping in the US High Plains: A synthesis of observed streamflow changes, J. Hydrol., 390(3–4), 222–244, doi:10.1016/j.jhydrol.2010.06.045, 2010.

Kustu, M. D., Fan, Y. and Rodell, M.: Possible link between irrigation in the U.S. High Plains and increased summer streamflow in the Midwest, Water Resour. Res., 47(3), doi:10.1029/2010WR010046, 2011.

Labat, D., Goddéris, Y., Probst, J. L. and Guyot, J. L.: Evidence for global runoff increase related to climate warming, Adv. Water Resour., 27(6), 631–642, doi:10.1016/j.advwatres.2004.02.020, 2004.

Lawrence, D. and Vandecar, K.: Effects of tropical deforestation on climate and agriculture, Nat. Clim. Chang., 5(1), 27–36, doi:10.1038/nclimate2430, 2014.

Legates, D. R., Lins, H. F. and McCabe, G. J.: Comments on “Evidence for global runoff increase related to climate warming” by Labat et al., Adv. Water Resour., 28(12), 1310–1315, doi:10.1016/j.advwatres.2005.04.006, 2005.

Matin, M. A. and Bourque, C. P.-A.: Relating seasonal dynamics of enhanced vegetation index to the recycling of water in two endorheic river basins in north-west China, Hydrol. Earth Syst. Sci., 19(8), 3387–3403, doi:10.5194/hess-19-3387-2015, 2015.

Milliman, J. D., Farnsworth, K. L., Jones, P. D., Xu, K. H. and Smith, L. C.: Climatic and anthropogenic factors affecting river discharge to the global ocean, 1951–2000, Glob. Planet. Change, 62(3), 187–194, doi:10.1016/j.gloplacha.2008.03.001, 2008.

Monteith, J. L.: Evaporation and environment, in Symp Soc Exp Biol, vol. 19, pp. 205–234, Cambridge University Press, Swansea., 1965.

Nitzbon, J., Heitzig, J. and Parlitz, U.: Sustainability, collapse and oscillations of global climate, population and economy in a simple World-Earth model, Environ. Res. Lett., doi:10.1088/1748-9326/AA7581, 2017.

Piao, S., Friedlingstein, P., Ciais, P., de Noblet-Ducoudré, N., Labat, D. and Zaehle, S.: Changes in climate and land use have a larger direct impact than rising CO2 on global river runoff trends., Proc. Natl. Acad. Sci. U. S. A., 104(39), 15242–15247, doi:10.1073/pnas.0707213104, 2007.

Pitman, A. J., de Noblet-Ducoudré, N., Cruz, F. T., Davin, E. L., Bonan, G. B., Brovkin, V., Claussen, M., Delire, C., Ganzeveld, L., Gayler, V., van den Hurk, B. J. J. M., Lawrence, P. J., van der Molen, M. K., Müller, C., Reick, C. H., Seneviratne, S. I., Strengers, B. J. and Voldoire, A.: Uncertainties in climate responses to past land cover change: First results from the LUCID intercomparison study, Geophys. Res. Lett., 36(14), 1–6, doi:10.1029/2009GL039076, 2009.

Portmann, F. T., Siebert, S. and Döll, P.: MIRCA2000—Global monthly irrigated and rainfed crop areas around the year 2000: A new high-resolution data set for agricultural and hydrological modeling, Global Biogeochem. Cycles, 24(1), 1–24, doi:10.1029/2008GB003435, 2010.

Ramankutty, N. and Foley, J. A.: Estimating historical changes in global land cover: Croplands historical have converted areas, Global Biogeochem. Cycles, 13(4), 997–1027, 1999.

Ramankutty, N., Evan, A. T., Monfreda, C. and Foley, J. A.: Farming the planet: 1. Geographic distribution of global agricultural lands in the year 2000, Global Biogeochem. Cycles, 22(1), 1–19, doi:10.1029/2007GB002952, 2008.

Reyer, C. P. O., Brouwers, N., Rammig, A., Brook, B. W., Epila, J., Grant, R. F., Holmgren, M., Langerwisch, F., Leuzinger, S., Lucht, W., Medlyn, B., Pfeifer, M., Steinkamp, J., Vanderwel, M. C., Verbeeck, H. and Villela, D. M.: Forest resilience and tipping points at different spatio-temporal scales: Approaches and challenges, edited by D. Coomes, J. Ecol., 103(1), 5–15, doi:10.1111/1365-2745.12337, 2015.

Rost, S., Gerten, D., Bondeau, A., Lucht, W., Rohwer, J. and Schaphoff, S.: Agricultural green and blue water consumption and its influence on the global water system, Water Resour. Res., 44, W09405, doi:10.1029/2007WR006331, 2008a.

Rost, S., Gerten, D. and Heyder, U.: Human alterations of the terrestrial water cycle through land management, Adv. Geosci., 18(18), 43–50, doi:10.5194/adgeo-18-43-2008, 2008b.

Shepherd, T. G.: Atmospheric circulation as a source of uncertainty in climate change projections, Nat. Geosci., 7(10), 703–708, doi:10.1038/ngeo2253, 2014.

Spracklen, D. V. and Garcia-Carreras, L.: The impact of Amazonian deforestation on Amazon basin rainfall, Geophys. Res. Lett., 42, 9546–9552, doi:10.1002/2015GL066063, 2015.

Spracklen, D. V., Arnold, S. R. and Taylor, C. M.: Observations of increased tropical rainfall preceded by air passage over forests, Nature, 489(7415), 282–285, doi:10.1038/nature11390, 2012.

Sterling, S. M., Ducharne, A. and Polcher, J.: The impact of global land-cover change on the terrestrial water cycle, Nat. Clim. Chang., 3(4), 385–390, doi:10.1038/nclimate1690, 2012.

Stewart, J. .: Modelling surface conductance of pine forest, Agric. For. Meteorol., 43(1), 19–35, doi:10.1016/0168-1923(88)90003-2, 1988.

The MathWorks, I.: MATLAB 8.4, n.d.

Wang-Erlandsson, L., van der Ent, R. J., Gordon, L. J. and Savenije, H. H. G.: Contrasting roles of interception and transpiration in the hydrological cycle – Part 1: Temporal characteristics over land, Earth Syst. Dyn., 5(2), 441–469, doi:10.5194/esd-5-441-2014, 2014.

Wang-Erlandsson, L., Bastiaanssen, W. G. M., Gao, H., Jägermeyr, J., Senay, G. B., van Dijk, A. I. J. M., Guerschman, J. P., Keys, P. W., Gordon, L. J. and Savenije, H. H. G.: Global root zone storage capacity from satellite-based evaporation, Hydrol. Earth Syst. Sci., 20(4), 1459–1481, doi:10.5194/hess-20-

1459-2016, 2016.

Wei, Z., Yoshimura, K., Wang, L., Miralles, D. G., Jasechko, S. and Lee, X.: Revisiting the contribution of transpiration to global terrestrial evapotranspiration, Geophys. Res. Lett., 44(6), 2792–2801, doi:10.1002/2016GL072235, 2017.

Werth, D. and Avissar, R.: The local and global effects of Amazon deforestation, J. Geophys. Res., 107, 8087, doi:10.1029/2001JD000717, 2002.